TOXICOLOGICAL SCIENCES **105(1)**, 134–141 (2008)
doi:10.1093/toxsci/kfn103
Advance Access publication May 22, 2008

Probing Mechanisms of Axonopathy. Part I: Protein Targets of 1,2-Diacetylbenzene, the Neurotoxic Metabolite of Aromatic Solvent 1,2-Diethylbenzene

Desire Tshala-Katumbay,*,‡,[1] Victor Monterroso,† Robert Kayton,‡ Michael Lasarev,‡ Mohammad Sabri,*,‡ and Peter Spencer*,‡

Department of Neurology; †Department of Comparative Medicine, School of Medicine; and ‡Center for Research on Occupational & Environmental Toxicology, Oregon Health & Science University, 3181 SW Sam Jackson Park Road, Portland, Oregon 97239

Received April 4, 2008; accepted May 16, 2008

Motor neuron axonopathy in diseases such as amyotrophic lateral sclerosis can be modeled and probed with neurotoxic chemicals that induce similar patterns of pathology, such as axonal spheroids that represent focal accumulation of anterogradely transported neurofilaments (NFs). The aromatic γ-diketone–like 1,2-diacetylbenzene (1,2-DAB), but not its 1,3-DAB isomer, reacts with ε-amino- or sulfyhydryl groups of (neuro)proteins, forms adducts, and causes NFs to accumulate at proximal sites of elongate motor axons. We exploit the protein-reactive properties of neurotoxic 1,2-DAB versus the nonprotein-reactive properties of non-neurotoxic 1,3-DAB to unveil proteomic changes associated with this type of pathology. We used two-dimensional differential in-gel electrophoresis (2D-DIGE), matrix-assisted laser desorption/ionization time-of-flight tandem mass spectrometry to analyze the lumbosacral spinal cord proteome of adult Sprague-Dawley rats treated systemically with 20 mg/kg/day 1,2-DAB, equimolar dose of 1,3-DAB, or equivalent volume of vehicle (saline containing 2% acetone), 5 days a week, for 2 weeks. 1,2-DAB significantly altered the expression of protein disulfide isomerase, an enzyme involved in protein folding, and gelsolin, an actin-capping and -severing protein. Modifications of these two proteins have been incriminated in the pathogenesis of nerve fiber degeneration. Protein-reactive and neurotoxic 1,2-DAB appears to be excellent tool to dissect mechanisms of nerve fiber (axon) degeneration.

Key Words: **axonal swellings; γ-diketones; gelsolin; protein disulfide isomerase; proteomics; solvent neuropathy.**

Molecular mechanisms underlying motor neuron axonopathy in diseases such as amyotrophic lateral sclerosis (ALS) have yet to be understood. Pathological changes often occur in axons before nerve cell bodies suggesting the existence of axon-specific targets and/or mechanisms associated with neurodegeneration. For instance, an early pathological sign in ALS consists of intraspinal axonal spheroids filled with neurofilaments (NFs) and abnormal protein aggregates, whereas the full-blown picture of pathological changes (dying back-axons, inclusions in nerve cell bodies, and cell death) is seen late in the course of the disease (Kato, 2008). Focal accumulation of axonal NFs is also seen in rodent models of axonopathy induced by certain neurotoxic compounds, such as aliphatic γ-diketone 2,5-hexanedione (2,5-HD) or its aromatic cousin 1,2-diacetylbenzene (1,2-DAB) (Spencer *et al.*, 2002; Tshala-Katumbay *et al.*, 2005). Direct application of 2,5-HD to nerve fibers induces within minutes a reorganization of axoplasmic structures comparable to that seen in systemic intoxication with 1,2-DAB or 2,5-HD (Tshala-Katumbay *et al.*, 2005; Zagoren *et al.*, 1983), which suggests the targets of these agents reside within the axon.

We and others have suggested previously that aromatic 1,2-DAB and aliphatic 2,5-HD, but not their respective 1,3-DAB or 2,4-HD isomers, react with ε-amino- or sulfyhydryl (SH)-groups of (neuro)proteins, form adducts, and promote protein cross-linking and polymerization (DeCaprio, 1986, 1987; Kim *et al.*, 2002). We exploit the protein-reactive property of 1,2-DAB versus the nonprotein-reactive property of 1,3-DAB to unveil proteomic changes associated with axonopathy. We used a high-throughput proteomic methodology consisting of two-dimensional differential in-gel electrophoresis (2D-DIGE) followed by protein identification (ID) by matrix-assisted laser desorption ionization time-of-flight/tandem mass spectrometry (MALDI-TOF/MS-MS) to analyze the lumbar spinal cord proteome of adult male Sprague-Dawley rats systemically treated with 1,2-DAB. We show that 1,2-DAB modifies the expression of proteins and/or enzymes involved in protein folding, maintaining axonal shape and dimensions, detoxification and redox mechanisms, and in supporting energy metabolism. Our approach has identified novel actors in the play performed by 1,2-DAB, including protein disulfide isomerase (PDI), an enzyme that modulates protein folding, and gelsolin, an actin-capping and -severing protein.

[1] To whom correspondence should be addressed at Center for Research on Occupational and Environmental Toxicology, Oregon Health & Science University, 3181 S.W. Jackson Park Road, mail code L606, Portland, OR 97239. Fax: (503) 494-6831. E-mail: tshalad@ohsu.edu.

METHODS

Chemicals

1,2-DAB (99%) and its isomer 1,3-DAB (97%) were purchased from Aldrich Chemical Co. (Madison, WI) and desiccated at room temperature (1,2-DAB) or stored at 4°C (1,3-DAB). Stock samples were checked by gas chromatography–mass spectrometry to confirm the purity of the chemicals. Impurities could not be readily identified, but 1,3-DAB was found to be free of 1,2-DAB and vice versa.

Animals

Experiments were conducted with male Sprague-Dawley rats (Charles Rivers, CA) weighing 175–225 g upon arrival. Animals were individually caged and given rodent chow (PMI Nutrition International, NJ) and water *ad libitum*. They were acclimated for 5 days in a room maintained at 20°C on a 12-h/12-h light-dark cycle prior to the commencement of the study.

Treatment of Animals

Rats were treated with 20 mg/kg/day 1,2-DAB ($n = 5$), 1,3-DAB ($n = 5$), or an equivalent volume of vehicle (saline containing 2% acetone) ($n = 5$), 5 days a week, for 2 weeks. Agents were administered intraperitoneally with a 1-ml disposable plastic syringe equipped with a 27-gauge needle. Injection sites were rotated around the abdomen and care was taken to minimize leakage and discomfort. Animals were observed daily for changes in behavior, physical appearance, and locomotion in an open field before and after treatment. They were also weighed before treatment to track changes in body weight and adjust the daily dose of the chemicals.

Tissue Preparation

At study termination, rats ($n = 3$ per treatment group) were anesthetized with 4% isofluorane (0.7 l oxygen/min), their blood collected via cardiac puncture, and then decapitated prior to the removal of the spinal cord. The spinal cord was removed by pressurized saline extrusion, divided into two halves (cranial and caudal halves), and flash-frozen in liquid nitrogen and stored at –80°C prior to proteomic studies.

For morphological studies, the remaining animals were anesthetized as described above, the abdomen and chest opened, and the heart injected with 50 µl of heparin solution (1000 United States Pharmacopea units/ml). Immediately thereafter, the left atrium and ventricular apex were excised, a cannula spurting perfusate introduced and clamped into the ascending aorta, and the animal perfused with cold 4% paraformaldehyde followed by 5% glutaraldehyde, each in 0.2M sodium cacodylate buffer (pH 7.4). The lumbosacral spinal cord and sciatic nerve were sampled, postfixed in excess cacodylate-buffered 1% osmium tetroxide, dehydrated, and embedded in epoxy resin. Cross-sections (~900 nm) were stained with 1% toluidine blue and screened by bright-field microscopy. Thin sections (~90 nm) of regions of interest were stained with 2% uranyl acetate followed by 1% lead citrate for examination by transmission electron microscopy.

Proteomic Studies

Sample preparation. Flash-frozen rat lumbosacral spinal cords were shipped on dry ice to Applied Biomics (Hayward, CA) for proteomic studies. Tissues were washed three times in buffer containing 10mM Tris-HCl and 5mM magnesium acetate (pH 8.0) to remove contaminating blood prior to the commencement of proteomic experiments that were conducted independently three times. Thereafter, proteins were dissolved in 2-D lysis buffer (30mM Tris-HCl, pH 8.8, containing 7M urea, 2M thiourea, and 4% 3-[(3-Cholamidopropyl)dimethylammonio]-1-propanesulfonate (CHAPS)) and incubated at room temperature for 30 min on a shaker. The lysed tissue samples were centrifuged for 30 min at 16,000 × g. The supernatants were collected and the protein quantity was measured using the Bio-Rad protein assay kit (Bio-Rad, CA).

CyDye labeling. To label proteins, 30 µg of each protein samples were incubated with 0.7 ml of diluted CyDye (1:5 diluted in dimethylformamide from 1 nmol/ml stock, GE Healthcare, NJ) at 4°C for 30 min. The labeling was stopped by adding 0.7 ml of 10mM L-lysine and incubating at 4°C for 15 min. The labeled samples were mixed together, and equal volume of 2× 2-D sample buffer (8M urea, 4% CHAPS, 20 mg/ml DTT, 2% pharmalytes and trace amount of bromophenol blue) and 100 ml of destreak solution (GE Healthcare) were added. The total sample volumes were adjusted to 260 ml by adding rehydration buffer (7M urea, 2M thiourea, 4% CHAPS, 20 mg/ml dithiotreitol [DTT], 1% pharmalytes and trace amount of bromophenol blue). The samples were incubated at room temperature for 10 min on a shaker and centrifuged for 10 min at 16,000 × g. The supernatants were loaded onto a 13-cm immobilized pH gradient gel (IPG) strip holder (GE Healthcare) prior to isoelectric focusing (IEF) and sodium dodecyl sulfate–polyacrylamide gel electrophoresis (SDS-PAGE).

IEF and SDS-PAGE. Thirteen-centimeter IPG strips (pH 3–10) were put on the loaded samples and 1 ml of mineral oil added on top of the strips. IEF was run according to the protocol provided by the manufacturer (GE Healthcare). Upon completion of the IEF, the IPG strips were incubated in freshly made equilibration buffer 1 (50mM Tris-HCl, pH 8.8, containing 6M urea, 30% glycerol, 2% SDS, trace amount of bromophenol blue, and 10 mg/ml DTT) for 15 min with gentle shaking. Thereafter, they were rinsed in the equilibration buffer 2 (50mM Tris-HCl, pH 8.8, containing 6M urea, 30% glycerol, 2% SDS, trace amount of bromophenol blue, and 45 mg/ml DTT) for 10 min with gentle shaking, and 1× in the SDS-gel running buffer prior to their transfer onto gradient SDS-gels (9–12%) prepared using low fluorescent glass plates and sealed with 0.5% (wt/vol) agarose solution (in SDS-gel running buffer). The SDS-gels were run at 15°C and stopped when the front dye had run out of the gels.

Image scan and software analysis. Gel scanning was carried out immediately after the SDS-PAGE using Typhoon TRIO (Amersham Biosciences, NJ). Scanned images were analyzed by Image Quant software (version 5.0, Amersham Biosciences) and subjected to in-gel analysis and cross-gel analysis using the DeCyder software (version 6.0, GE Healthcare) with a detection limit of 0.2 ng of protein per spot. The ratio change for differentially expressed protein spots was obtained from the in-gel DeCyder analysis.

Preparative gel and spot picking for mass spectrometry. A total of 600–700 µg of unlabeled proteins was run in a preparative gel and stained with Deep Purple total protein stain (GE Healthcare) prior to mass spectrometry analysis. Twenty-two protein spots that were consistently differentially expressed in 1,2-DAB- versus vehicle- and 1,3-DAB-treated samples across a minimum of two gels were picked up by the Ettan Spot Picker (GE Healthcare) and subjected to in-gel trypsin digestion, peptide extraction, and desalting prior to MALDI-TOF/MS-MS.

In-gel digestion, mass spectrometry, and database search. Proteins of interest were digested in-gel with modified porcine trypsin protease (Trypsin Gold, Promega, WI). The digested tryptic peptides were desalted by Zip-tip C18 (Millipore, CA). Peptides were eluted from the Zip-tip with 0.5 µl of matrix solution (α-cyano-4-hydroxycinnamic acid (5 mg/ml in 50% acetonitrile, 0.1% trifluoroacetic acid, 25mM ammonium bicarbonate) and spotted on the MALDI plate (model ABI 01-192-6-AB). MALDI-TOF MS and TOF/TOF tandem MS/MS were performed on an ABI 4700 mass spectrometer (Applied Biosystems, CA). MALDI-TOF mass spectra were acquired in reflectron positive ion mode, averaging 4000 laser shots per spectrum. TOF/TOF tandem MS fragmentation spectra were acquired for each protein, averaging 4000 laser shots per fragmentation spectrum on each of the 10 most abundant ions present in each sample (excluding trypsin autolytic peptides and other known background ions). Both the resulting peptide mass and the associated fragmentation spectra were submitted to GPS Explorer workstation equipped with MASCOT search engine (Matrix science, MA) to search the National Center for Biotechnology Information nonredundant databases. Searches were performed without constraining protein molecular weight or isoelectric point, with variable carbamidomethylation of cysteine and oxidation of methionine residues, and with one missed cleavage also allowed in the search parameters.

Candidates with protein- and ion-confidence score(s) greater than 95% were considered significant.

Statistical Analysis

Each animal's body weight was measured five times per week for 2 weeks and was summarized by fitting a linear trend to the series of body weight measurements. The estimated slope coefficient from each fit reflects the change in body weight per day. Nonparametric procedures (Kruskall-Wallis, Wilcoxon rank-sum) were used to determine whether the slope coefficients differed among the three groups. All computations were performed using R version 2.6.1 (R Development Core Team, 2007).

Changes in number of protein spots that were differentially expressed were analyzed using log-linear models with an allowance made for overdispersion.

RESULTS

Physical and Neuropathological Changes

Rats treated with 1,2-DAB, but not with 1,3-DAB or vehicle, developed neuromuscular hind limb weakness together with postural and gait abnormalities. These signs occurred after ~1 week of treatment with 1,2-DAB. Daily changes in body weight significantly differed among the three groups of animals treated with 1,2-DAB, or 1,3-DAB, or vehicle (χ^2 (2df) = 9.42, $p = 0.01$; Kruskal-Wallis test). There was no difference in body weight changes between 1,3-DAB- and vehicle-treated animals ($W = 14$, $p = 0.84$). These two groups typically gained 9.9 g/day ($W = 55$, $p = 0.002$; 95% CI: 8.7–11.2 g/day). Relative to animals treated with either 1,3-DAB or vehicle, those given 1,2-DAB lost approximately 14 g/day more weight ($W = 50$, $p < 0.001$; 95% CI: 10.8–19.1 g/day more weight lost) (Table 1).

Only animals treated with 1,2-DAB showed nerve fiber damage. Light microscopy of the lumbar spinal cord revealed 10-nm NF-filled swollen axons in spinal cord anterior horns and proximal ventral roots. Neurons in the adjacent dorsal horns were unremarkable. Electron microscopy of enlarged axons revealed disorganization of the cytoskeleton in the form of clustering of microtubules and organelles and NF segregation. In some instances, NF accumulated inside the nerve cell bodies (Fig. 1).

TABLE 1
Estimated Change in Body Weight (g) per Day (i.e., Slope Coefficient) for Each of the Five Animals in each Treatment Group

Vehicle-treated animals	1,3-DAB-treated animals	1,2-DAB-treated animals
7.35	7.68	−10.28
8.79	9.08	−6.69
10.27	9.75	−3.14
12.18	10.85	−2.16
12.41	10.94	−0.93

Proteomic Changes

The Decyder analysis of protein expression across the proteomic experiments revealed that both 1,2-DAB and 1,3-DAB induced changes in expression levels of proteins. However, axonopathic1,2-DAB induced greater change in protein expression relative to 1,3-DAB and/or vehicle. For example, relative to 1,3-DAB, the effect of 1,2-DAB was to significantly *increase* the number of protein spots showing both "increased" and "decreased" protein expression ($p < 0.001$). The number of spots with high or low expression levels was 3.2 times higher (95% CI: 1.6–6.5 times higher) or 2.4 times higher (95% CI: 1.4–4.2 times higher), respectively, in 1,2-DAB- versus vehicle-treated relative to 1,3-DAB- versus vehicle-treated animals (Table 2, Fig. 2). The observed changes in protein expression were consistent across the gels ($p = 0.82$) suggesting reliable conditions and results across the proteomic experiments.

After visual inspection of fluorescent images of analytical gels, 22 protein spots were classified independently by two experienced neuroscientists blind to the experimental conditions as being markedly altered by treatment with 1,2-DAB relative to 1,3-DAB and vehicle (spots 1–22, Fig. 3 and Table 3). Mass spectrometry ID of these 22 protein spots revealed proteins and/or enzymes that are involved in protein folding (e.g., PDI), maintaining axonal shape and dimensions (e.g., NF-L or gelsolin), detoxification and redox mechanisms (e.g., glutathione-*S* transferase), and supporting energy metabolism (e.g., ATP citrate lyase). Novel findings in the pathogenesis of γ-diketone axonopathy included the downregulation of gelsolin and PDI (spots 5 and 9 in Fig. 3 and Table 3, Fig. 4). We studied the mRNA expression of NF-L, gelsolin, and PDI and showed no transcriptional changes. To validate our proteomic findings, we have confirmed changes in the expression level of a selected protein, that is, PDI using Western blot (data not shown).

DISCUSSION

This is the first study to report on global proteomic changes associated with proximal giant neurofilamentous axonopathy induced by the γ-diketone–like 1,2-DAB. We have identified 22 proteins that were remarkably altered by treatment with axonopathic 1,2-DAB relative to its nonaxonopathic isomer 1,3-DAB or vehicle. Novel findings include downregulation of PDI, a chaperone molecule that regulates protein folding and of gelsolin, an actin-capping and -severing protein with yet unresolved antiapoptotic properties (Endres *et al*., 1999; Ferrari and Soling, 1999; Furukawa *et al*., 1997; Harms *et al*., 2004; Maattanen *et al*., 2006). Whether the change in expression levels of PDI and gelsolin are linked is unknown, but it is possible they are coupled upstream and downstream effects of 1,2-DAB, the former triggering protein misfolding and the latter reflecting activation of protein degradation. Whether the

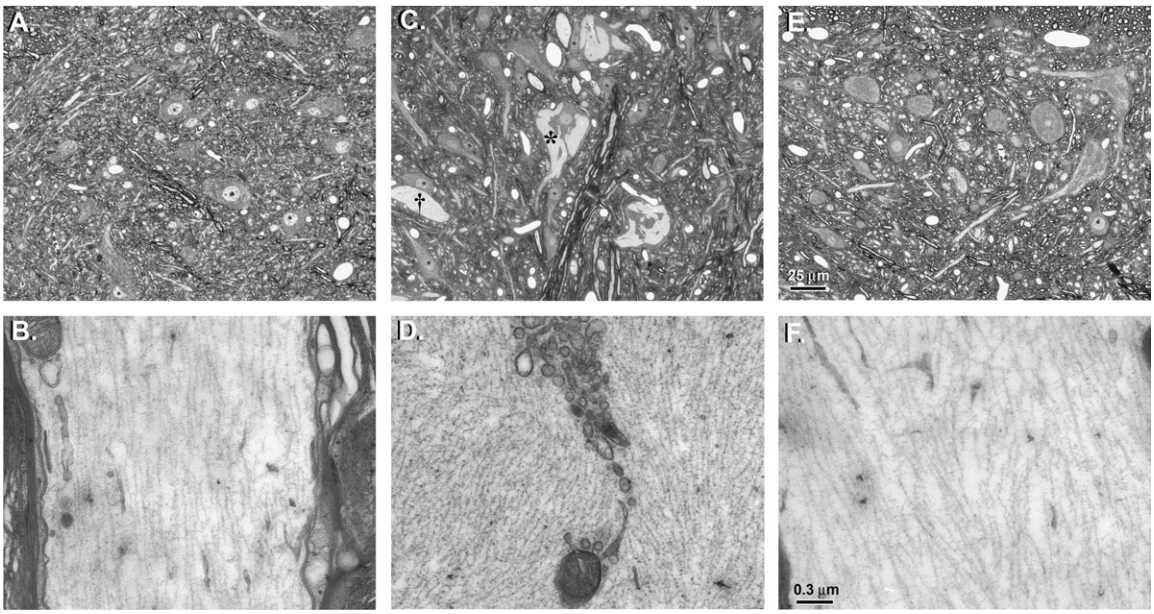

FIG. 1. Cross-sections of lumbar spinal cords of rats treated i.p. with vehicle (A and B), 20 mg/kg/day 1,2-DAB (C and D), or 1,3-DAB (E and F), 5 days a week, for 2 weeks. The upper panel shows light-microscope images and the lower panel are the corresponding electron microscopy images. Hypochromic zones (*) corresponding to NF accumulation in anterior horn cells and giant axonal swellings (†) were evident in animals treated with 1,2-DAB (C). Electron microscopy of this region revealed disorganization of the cytoskeleton and clustering of organelles in axonal swellings that were densely packed with NF (D). Spinal cords from animals treated with vehicle (A, B) or 1,3-DAB (E, F) were unremarkable. Cross-sections (~900 nm) for light microscopy were stained with 1% toluidine blue. Thin sections (~90 nm) of regions of interest were stained with 2% uranyl acetate followed by 1% lead citrate for transmission electron microscopy.

change in PDI expression is associated with changes in metabolism and function of the endoplasmic reticulum, the main host-organelle of PDI, is another relevant question (Atkin *et al*., 2006; Bertoli *et al*., 2004; Ferrari and Soling, 1999).

PDI could conceivably play a critical role in the pathogenesis of γ-diketone axonopathy for several reasons. First, its abundant lysine content (9.9% of total amino acid) makes PDI highly vulnerable to chemical attack by γ-diketones. Second, four of six γ-diketone–vulnerable cysteine residues (SH-group carriers) are located on the two PDI redox active sites that participate in disulfide bond formation and maintenance of the 3D-conformation of the molecule. Third, modification (adduction) of PDI could result in downstream effects on protein-protein interaction, perhaps resulting in changes in cytoskeletal disorganization of the type seen after local and/or systemic treatment with 2,5-HD or 1,2-DAB (Zagoren *et al*., 1983; Tshala-Katumbay *et al*., 2005). Fourth, changes in PDI expression/activity might prevent proper folding of nascent cytoskeleton proteins. For example, NF proteins synthesized in the anterior horn cell and destined for transport to the axon might lose their binding properties and accumulate in proximal axonal spheroids or even fail to exit the cell body. It is noteworthy that changes in PDI expression and its *S*-nitrosylation have been proposed to play a role in the pathogenesis of neurodegenerative diseases such as the ALS, which has axonal spheroids indistinguishable from those induced by 1,2-DAB (Atkin *et al*., 2006; Kozarova *et al*., 2007; Nakamura and Lipton, 2008). We suggest that more studies are conducted to understand the role of PDI and that of redox assistants in protein folding (glutathione and Ero-1) (Atkin *et al*., 2006; Bertoli *et al*., 2004; Cuozzo and Kaiser, 1999; Molteni *et al*., 2004) in the pathogenesis of γ-diketone axonopathy.

TABLE 2
Number of Protein Spots Identified by the Decyder Software as being Differentially Expressed in 1,2-DAB or 1,3-DAB Relative to Vehicle-Treated Samples

	1,2-DAB versus vehicle			1,3-DAB versus vehicle		
Protein expression	Gel 1	Gel 2	Gel 3	Gel 1	Gel 2	Gel 3
Decreased	134	90	114	28	35	77
Increased	99	90	58	16	42	19
Unchanged	1246	1268	1223	1435	1371	1299

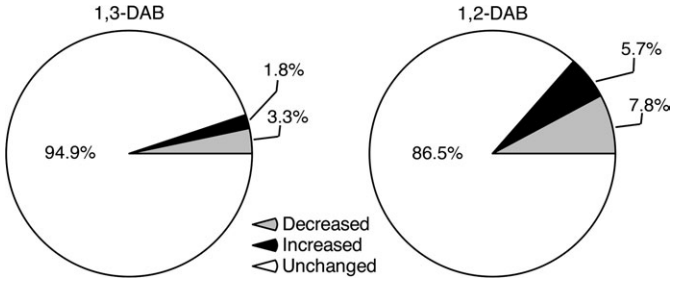

FIG. 2. Average proportion of protein spots differentially expressed in 1,3-DAB- versus vehicle-treated samples (left) and 1,2-DAB- versus vehicle-treated samples (right). Relative to 1,3-DAB, 1,2-DAB significantly altered (increased or decreased) the expression levels of proteins.

Gelsolin is another novel protein actor in 1,2-DAB axonopathy that for several reasons may have mechanistic importance in the genesis of motor neuron/axon pathology. First, it modulates the formation (polymerization-depolymerization) of the actin (microfilament) network. Changes in gelsolin expression and/or activity might disrupt the interactions and/or the structural organization of the cytoskeleton, resulting for example in the separation of NFs and microtubules seen in early stages of γ-diketone axonopathy. Second, gelsolin is implicated in regulating apoptotic cell death, a phenomenon that has been reported in cell cultures treated with γ-diketones but that has still to be demonstrated *in vivo*. And third, mutation in the gene that codes for gelsolin has been linked to the pathogenesis of the Finnish type familial amyloid polyneuropathy, a neurodegenerative disease with mechanisms that have yet to be understood (Harms *et al*., 2004; Ikeda *et al*., 2007; Roch *et al*., 2007; Spinardi and Witke, 2007; Tanskanen *et al*., 2007).

Several other proteins were selectively altered in animals treated with 1,2-DAB versus 1,3-DAB or vehicle. NF-L showed a reduced expression that was unexpected in the absence of comparable reductions in NF-H, which has higher lysine content and in mutated form has been implicated in a rare familial form of ALS (Al-Chalabi *et al*., 1999; Robberecht, 2000). However, NF may be bystanders in the genesis of γ-diketone axonopathy because knocking out the genes that code for NF proteins does not affect susceptibility to 2,5-HD, the aliphatic γ-diketone cousin of 1,2-DAB (Sickles *et al*., 1994; Stone *et al*., 2001). Proteins or enzymes associated with energy metabolism have been previously implicated in the genesis of γ-diketone axonopathy (Sabri *et al*., 1979; Sabri, 1984) and were well represented (ACLY, Hadha, ODP2, Pkm2, Hmgcs1, Ndufa10, and Gpd) among the 22 proteins studied here. ACLY activity was proposed as a biomarker of Wallerian degeneration in peripheral nerves in the late 60′s (Bonavita *et al*., 1968). Pkm2 and Hadha, a subunit of the mitochondrial trifunctional protein (TFP), may also be of interest because mutations in the genes encoding for TFP subunits and oxidative damage of pkm2 have been respectively implicated in systemic organ failure associated with encephalopathy and mild cognitive impairment in aging subjects (Butterfield *et al*., 2006; Choi *et al*., 2007). Changes in the expression level of Gstm1 may be related to an initiation of a detoxification process (Brock *et al*., 1981; Coles *et al*., 1984). It is not known whether regulation of Blvrd and Dhpr, which influence nicotinamide adenine dinucleotide phosphate, reduced (NADPH) metabolism, may trigger an oxidative response (Armarego *et al*., 1984; Florczyk *et al*., 2008; Sun *et al*., 2007). Oxidative damage has been recently proposed in the genesis of 1,2-DAB axonopathy in cell cultures (Kim *et al*., 2007). However, the underlying mechanisms and whether this occurs *in vivo* have yet to be elucidated. Whether changes in expression levels of endoplasmin, a heat shock protein and/or Gdi2, a protein involved in intracellular trafficking of vesicles

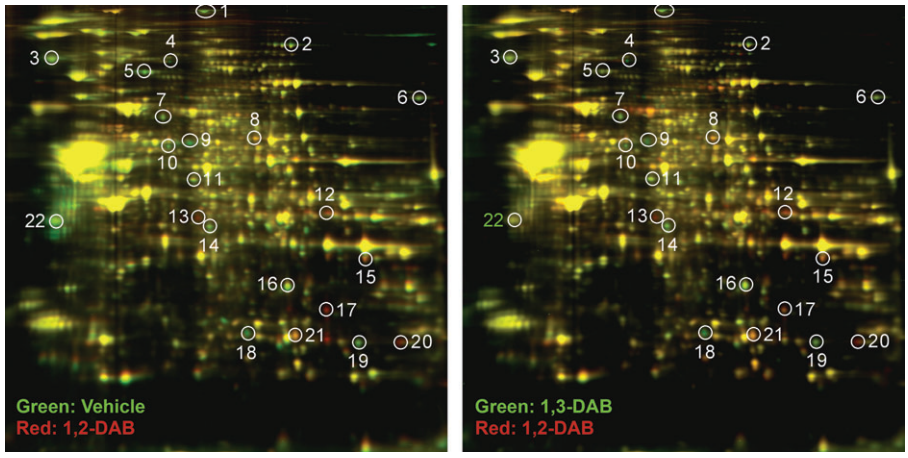

FIG. 3. Representative 2D-DIGE patterns of lumbar spinal cords from animals treated with 20 mg/kg/day 1,2-DAB versus 1,3-DAB, 5 days a week, for 2 weeks. The 22 differentially expressed protein spots (circles 1–22) that were differentially modulated by 1,2-DAB versus vehicle (left) and 1,2-DAB versus 1,3-DAB (right) were subjected to MALDI-TOF/MS-MS for protein ID.

TABLE 3
List of Proteins Differentially Affected by 1,2-DAB (100% Confidence Score for Protein ID by MALDI-TOF/MS-MS)

Spot number	Protein name	Symbols	Accession number	Molecular weight	Isoelectric point	Peptides matched	Function	Fold change[a]
1	Fatty acid synthase	Fasn	204099	272,493.9	5.96	27	Metabolism of lipids	−1.65
2	ATP citrate lyase	Acly	8392839	120,558.7	6.96	23	Energy metabolism	−1.57
3	Endoplasmin		51858886	74,161.6	5.02	26	Heat shock protein	−1.44
4	Formyltetrahydrofolate dehydrogenase	Fthfd	57921067	98,811.5	5.64	34	Detoxification	−2.52
5	Gelsolin	Gsn	51854227	86,014.1	5.76	16	Protein binding/structural protein	−2.42
6	Hydroxyacyl-coenzyme A dehydrogenase/3-ketoacyl-coenzyme A thiolase/enoyl-coenzyme A hydratase (TFP), alpha subunit	Hadha	60688124	82612.5	9.16	22	Energy metabolism	−1.69
7	Dihydrolipoamide acetyltransferase	Odp2	34863356	67,123.4	8.76	12	Energy metabolism	−1.63
8	Pyruvate kinase muscle	Pkm2	56929	57,780.9	6.63	18	Energy metabolism	+2.02
9	PDI related 3	Pdi	38382858	56,587.7	5.88	20	Protein folding	−2.86
10	3-Hydroxy-3-methylglutaryl-coenzyme A synthase 1 (Hmgcs1)		8393538	57,397.4	5.58	16	Energy metabolism	−2.87
11	GDP dissociation inhibitor 2	Gdi2	40254781	50,504.7	5.93	18	Catalytic activity/vesicle trafficking	−1.19
12	Aldolase A	Aldoa	6978487	39,327.3	8.31	14	Catalytic activity	+1.85
13	NADH dehydrogenase (ubiquinone) 1 alpha	Ndufa10	46391108	31,680.8	5.44	9	Energy metabolism	+2.39
14	NADH dehydrogenase (ubiquinone) 1 alpha	Ndufa10	46391108	31,680.8	5.44	12	Energy metabolism	−1.83
15	Glyceraldehyde-3-phosphate dehydrogenase	Gpd	56611127	35,771.2	8.14	6	Energy metabolism	+1.38
16	Voltage-dependent anion channel-like protein	—	540011	31,699.6	7.44	7	Unknown	−2.1
17	Glyceraldehyde-3-phosphate dehydrogenase	Gpd	8393418	35,805.2	8.14	7	Energy metabolism	+6.8
18	Similar to biliverdin reductase B (flavin reductase)	Blvrd	34855391	22,080.3	6.29	9	NADPH diaphorase activity	−2.9
19	Glutathione-*S* transferase Yb-1 subunit (EC 2.5.1.18)	Gstm1	204503	25,899	7.63	13	Detoxification	−5.24
20	Glutathione-*S* transferase Yb-1 subunit (EC 2.5.1.18)	Gstm1	204503	25,899	7.63	17	Detoxification	+2.49
21	Quinoid dihydropteridine reductase	Dhpr	11693160	25,535.9	7.67	9	NADPH dihydropteridine reductase activity	+1.89
22	NF, light polypeptide	Nefl	13929098	61,298	4.63	17	Protein binding/structural protein	−1.61

[a]Maximum fold change values observed after cross-gel analysis of proteomic expression. Negative or positive values indicate low or high expression level, respectively, of the indicated protein in samples treated with neurotoxic 1,2-DAB. Dual protein expression of certain proteins (e.g., NADH) may possibly be explained by a concomitant expression of isoforms, or protein subunits, or post-translationally modified proteins. Protein no. 16 has been removed from the nrNCBI databases.

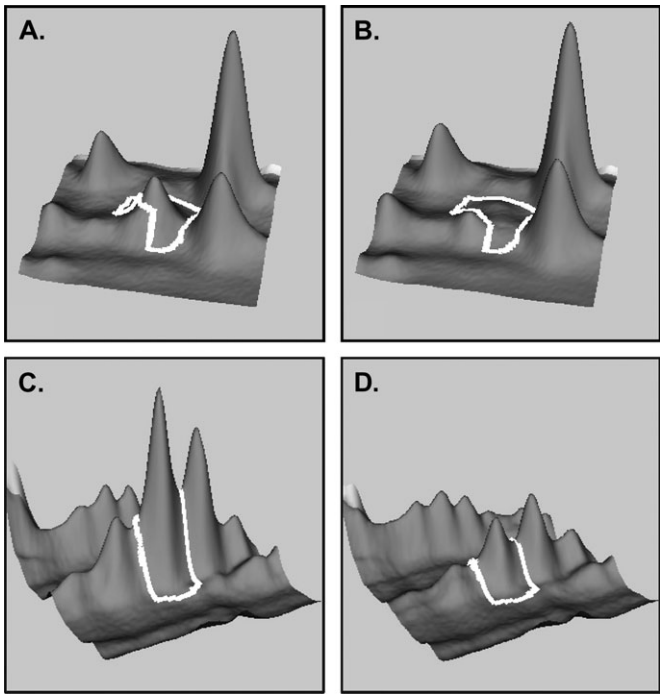

FIG. 4. DeCyder display of relative abundance of gelsolin and PDI. Upper pair: relative abundance of gelsolin (spot no. 5). Gelsolin showed 2.42× higher abundance in vehicle (A) relative to 1,2-DAB (B) treated sample. Lower pair: relative abundance of PDI (spot no. 9). PDI showed 2.86× higher abundance in vehicle—(C) relative to 1,2-DAB—(D) treated sample.

(Rivero *et al*., 2002; Shisheva *et al*., 1999), are related to 1,2-DAB treatment is also unknown and needs to be investigated.

Although the known functional properties of the 22 proteins are important to consider in relation to the genesis of motor neuron degeneration, there is an abundant need for caution in interpreting the findings. First and foremost, the proteins derive from whole spinal cord tissue, which represents a mixture of neuronal, glial and other cells. Second, the 22 selected proteins undoubtedly represent a fraction of the totality of protein changes and experimentation was done on a limited number of animals. Third, changes in protein expression may arise from the direct effects of 1,2-DAB in adducting proteins, from changes in protein breakdown or in protein synthesis, or in combinations of the foregoing. Changes in protein synthesis are unlikely to be responsible for the segregation of microtubules from NF seen in gamma-diketone axonopathy because this phenomenon is observed immediately following application of 2,5-HD to the sciatic nerve (Zagoren *et al*., 1983). We have found unaltered mRNA expression levels of PDI, NF-L and gelsolin (data not shown) suggesting that changes in expression of cytoskeleton proteins is unlikely to be caused by a decrease in protein synthesis but may be associated with either protein fragmentation and/or enzymatic degradation. Increase in expression levels of certain proteins may reflect the initiation of homeostatic and/or repair mechanisms following intoxication with 1,2-DAB.

Taken in concert, our global proteomic approach has revealed proteins that are selectively involved in the pathogenesis of 1,2-DAB axonopathy. Changes in PDI are most intriguing because of its established role in the maintenance of the three-dimensional structure of proteins required for normal enzymatic and other functions. Observed changes in the expression of cytoskeletal proteins (gelsolin) could be a downstream effect of alterations in PDI expression. Changes in gelsolin expression could affect cytoskeletal integrity, an early and perhaps key pathological event that precedes development of axonal spheroids.

FUNDING

National Institute of Health (K01NS052183, P42ES10338, U19ES11384); and Oregon Worker Benefit Fund.

ACKNOWLEDGMENTS

The technical expertise of Dan Austin (OHSU, Portland OR) and the guidance of Paul Desjardin and Roger Butterworth (Université de Montréal, Canada) are appreciated.

REFERENCES

Al-Chalabi, A., Andersen, P. M., Nilsson, P., Chioza, B., Andersson, J. L., Russ, C., Shaw, C. E., Powell, J. F., and Leigh, P. N. (1999). Deletions of the heavy neurofilament subunit tail in amyotrophic lateral sclerosis. *Hum. Mol. Genet.* **8,** 157–164.

Armarego, W. L., Randles, D., and Waring, P. (1984). Dihydropteridine reductase (DHPR), its cofactors, and its mode of action. *Med. Res. Rev.* **4,** 267–321.

Atkin, J. D., Farg, M. A., Turner, B. J., Tomas, D., Lysaght, J. A., Nunan, J., Rembach, A., Nagley, P., Beart, P. M., Cheema, S. S., *et al*. (2006). Induction of the unfolded protein response in familial amyotrophic lateral sclerosis and association of protein-disulfide isomerase with superoxide dismutase 1. *J. Biol. Chem.* **281,** 30152–30165.

Bertoli, G., Simmen, T., Anelli, T., Molteni, S. N., Fesce, R., and Sitia, R. (2004). Two conserved cysteine triads in human Ero1alpha cooperate for efficient disulfide bond formation in the endoplasmic reticulum. *J. Biol. Chem.* **279,** 30047–30052.

Bonavita, V., Piccoli, F., and Serra, S. (1968). Acetyl-CoA synthetase, NADP malate dehydrogenase and ATP citrate lyase in the degenerating peripheral nerve. *Brain Res.* **10,** 245–251.

Brock, N., Pohl, J., and Stekar, J. (1981). Detoxification of urotoxic oxazaphosphorines by sulfhydryl compounds. *J. Cancer Res. Clin. Oncol.* **100,** 311–320.

Butterfield, D. A., Poon, H. F., St Clair, D., Keller, J. N., Pierce, W. M., Klein, J. B., and Markesbery, W. R. (2006). Redox proteomics identification of oxidatively modified hippocampal proteins in mild cognitive impairment: Insights into the development of Alzheimer's disease. *Neurobiol. Dis.* **22,** 223–232.

Choi, J. H., Yoon, H. R., Kim, G. H., Park, S. J., Shin, Y. L., and Yoo, H. W. (2007). Identification of novel mutations of the HADHA and HADHB genes in patients with mitochondrial trifunctional protein deficiency. *Int. J. Mol. Med.* **19,** 81–87.

Coles, B., Ketterer, B., Beland, F. A., and Kadlubar, F. F. (1984). Glutathione conjugate formation in the detoxification of ultimate and proximate carcinogens of N-methyl-4-aminoazobenzene. *Carcinogenesis* **5,** 917–920.

Cuozzo, J. W., and Kaiser, C. A. (1999). Competition between glutathione and protein thiols for disulphide-bond formation. *Nat. Cell Biol.* **1,** 130–135.

DeCaprio, A. P. (1986). Mechanisms of in vitro pyrrole adduct autooxidation in 2,5-hexanedione-treated protein. *Mol. Pharmacol.* **30,** 452–458.

DeCaprio, A. P. (1987). n-Hexane neurotoxicity: A mechanism involving pyrrole adduct formation in axonal cytoskeletal protein. *Neurotoxicology* **8,** 199–210.

Endres, M., Fink, K., Zhu, J., Stagliano, N. E., Bondada, V., Geddes, J. W., Azuma, T., Mattson, M. P., Kwiatkowski, D. J., and Moskowitz, M. A. (1999). Neuroprotective effects of gelsolin during murine stroke. *J. Clin. Invest.* **103,** 347–354.

Ferrari, D. M., and Soling, H. D. (1999). The protein disulphide-isomerase family: Unravelling a string of folds. *Biochem. J.* **339,** 1–10.

Florczyk, U. M., Jozkowicz, A., and Dulak, J. (2008). Biliverdin reductase: New features of an old enzyme and its potential therapeutic significance. *Pharmacol. Rep.* **60,** 38–48.

Furukawa, K., Fu, W., Li, Y., Witke, W., Kwiatkowski, D. J., and Mattson, M. P. (1997). The actin-severing protein gelsolin modulates calcium channel and NMDA receptor activities and vulnerability to excitotoxicity in hippocampal neurons. *J. Neurosci.* **17,** 8178–8186.

Harms, C., Bosel, J., Lautenschlager, M., Harms, U., Braun, J. S., Hortnagl, H., Dirnagl, U., Kwiatkowski, D. J., Fink, K., and Endres, M. (2004). Neuronal gelsolin prevents apoptosis by enhancing actin depolymerization. *Mol. Cell Neurosci.* **25,** 69–82.

Ikeda, M., Mizushima, K., Fujita, Y., Watanabe, M., Sasaki, A., Makioka, K., Enoki, M., Nakamura, M., Otani, T., Takatama, M., and Okamoto, K. (2007). Familial amyloid polyneuropathy (Finnish type) in a Japanese family: Clinical features and immunocytochemical studies. *J. Neurol. Sci.* **252,** 4–8.

Kato, S. (2008). Amyotrophic lateral sclerosis models and human neuropathology: Similarities and differences. *Acta Neuropathol.* **115,** 97–114.

Kim, M. K., Kim, K. S., Chung, J. H., Kim, J. H., Kim, J. R., Chung, H. Y., and Kim, M. S. (2007). Environmental metabolite, 1,2-diacetylbenzene, produces cytotoxicity through ROS generation in HUVEC cells. *J. Toxicol. Environ. Health A* **70,** 1336–1343.

Kim, M. S., Hashemi, S. B., Spencer, P. S., and Sabri, M. I. (2002). Amino acid and protein targets of 1,2-diacetylbenzene, a potent aromatic gamma-diketone that induces proximal neurofilamentous axonopathy. *Toxicol. Appl. Pharmacol.* **183,** 55–65.

Kozarova, A., Sliskovic, I., Mutus, B., Simon, E. S., Andrews, P. C., and Vacratsis, P. O. (2007). Identification of redox sensitive thiols of protein disulfide isomerase using isotope coded affinity technology and mass spectrometry. *J. Am. Soc. Mass. Spectrom.* **18,** 260–269.

Maattanen, P., Kozlov, G., Gehring, K., and Thomas, D. Y. (2006). ERp57 and PDI: Multifunctional protein disulfide isomerases with similar domain architectures but differing substrate-partner associations. *Biochem. Cell. Biol.* **84,** 881–889.

Molteni, S. N., Fassio, A., Ciriolo, M. R., Filomeni, G., Pasqualetto, E., Fagioli, C., and Sitia, R. (2004). Glutathione limits Ero1-dependent oxidation in the endoplasmic reticulum. *J. Biol. Chem.* **279,** 32667–32673.

Nakamura, T., and Lipton, S. A. (2008). Emerging roles of s-nitrosylation in protein misfolding and neurodegenerative diseases. *Antioxid. Redox. Signal.* **10,** 87–102.

R Development Core Team. (2007). R: A language and environment for statistical computing. Available at: http://www.R-project.org. Accessed November 26, 2007.

Rivero, F., Illenberger, D., Somesh, B. P., Dislich, H., Adam, N., and Meyer, A. K. (2002). Defects in cytokinesis, actin reorganization and the contractile vacuole in cells deficient in RhoGDI. *EMBO J.* **21,** 4539–4549.

Robberecht, W. (2000). Genetics of amyotrophic lateral sclerosis. *J. Neurol.* **247,** 2–6.

Roch, J. A., Hermier, M., Jouvet, A., and Nighoghossian, N. (2007). [Cerebral amyloid angiopathy]. *Rev. Neurol. (Paris)* **163,** 134–137.

Sabri, M. I. (1984). In vitro effect of n-hexane and its metabolites on selected enzymes in glycolysis, pentose phosphate pathway and citric acid cycle. *Brain Res.* **297,** 145–150.

Sabri, M. I., Moore, C. L., and Spencer, P. S. (1979). Studies on the biochemical basis of distal axonopathies—I. Inhibition of glycolysis by neurotoxic hexacarbon compounds. *J. Neurochem.* **32,** 683–689.

Shisheva, A., Chinni, S. R., and DeMarco, C. (1999). General role of GDP dissociation inhibitor 2 in membrane release of Rab proteins: Modulations of its functional interactions by in vitro and in vivo structural modifications. *Biochemistry* **38,** 11711–11721.

Sickles, D. W., Pearson, J. K., Beall, A., and Testino, A. (1994). Toxic axonal degeneration occurs independent of neurofilament accumulation. *J. Neurosci. Res.* **39,** 347–354.

Spencer, P. S., Kim, M. S., and Sabri, M. I. (2002). Aromatic as well as aliphatic hydrocarbon solvent axonopathy. *Int. J. Hyg. Environ. Health* **205,** 131–136.

Spinardi, L., and Witke, W. (2007). Gelsolin and diseases. *Subcell. Biochem.* **45,** 55–69.

Stone, J. D., Peterson, A. P., Eyer, J., Oblak, T. G., and Sickles, D. W. (2001). Neurofilaments are nonessential to the pathogenesis of toxicant-induced axonal degeneration. *J. Neurosci.* **21,** 2278–2287.

Sun, G. Y., Horrocks, L. A., and Farooqui, A. A. (2007). The roles of NADPH oxidase and phospholipases A2 in oxidative and inflammatory responses in neurodegenerative diseases. *J. Neurochem.* **103,** 1–16.

Tanskanen, M., Paetau, A., Salonen, O., Salmi, T., Lamminen, A., Lindsberg, P., Somer, H., and Kiuru-Enari, S. (2007). Severe ataxia with neuropathy in hereditary gelsolin amyloidosis: A case report. *Amyloid* **14,** 89–95.

Tshala-Katumbay, D. D., Palmer, V. S., Kayton, R. J., Sabri, M. I., and Spencer, P. S. (2005). A new murine model of giant proximal axonopathy. *Acta Neuropathol. (Berl.)* **109,** 405–410.

Zagoren, J. C., Politis, M. J., and Spencer, P. S. (1983). Rapid reorganization of the axonal cytoskeleton induced by a gamma diketone. *Brain Res.* **270,** 162–164.